

# Femtosecond laser fabricated fiber Bragg grating in microfiber for refractive index sensing

X. Fang, C. R. Liao, and D. N. Wang\*

*Department of Electrical Engineering, The Hong Kong Polytechnic University, Hung Hom, Kowloon, Hong Kong, China*

\*Corresponding author: eednwang@polyu.edu.hk

Received November 18, 2009; revised February 2, 2010; accepted February 4, 2010;  
posted February 24, 2010 (Doc. ID 120188); published March 29, 2010

Fiber Bragg grating (FBG) is fabricated in the microfiber by the use of femtosecond laser pulse irradiation. Such a grating can be directly exposed to the surrounding medium without etching or thinning treatment of the fiber, thus possessing high refractive index (RI) sensitivity while maintaining superior reliability. The grating in the microfiber may have a number of propagation modes in its transmission spectrum, depending on the fiber diameter, and the higher order of mode has larger RI sensitivity. The RI sensitivity also depends on the fiber diameter and a smaller diameter corresponds to a large sensitivity. The maximum sensitivity obtained is  $\sim 231.4$  nm per refractive index unit at the refractive index value of  $\sim 1.44$  when the fiber diameter is  $\sim 2$   $\mu\text{m}$ . The FBG fabricated in the microfiber has high potential in various types of optical fiber sensor applications. © 2010 Optical Society of America

OCIS codes: 060.3735, 060.2370.

There has been increased research interest in optical microfibers/nanofibers in recent years [1–4] because of their many unique and interesting properties. An optical microfiber/nanofiber essentially consists of only fiber core, surrounded by air. When light travels along the fiber, it is tightly confined to the fiber core owing to the large refractive index (RI) contrast between the core and air, while a large fraction of the guided light can propagate outside the fiber as the evanescent wave, which makes it highly sensitive to the ambient medium. The small size of the microfiber/nanofiber also provides excellent flexibility and convenient configurability, allowing the easy manipulation of the microfiber-/nanofiber-based devices with a complex topology. Many microfiber-/nanofiber-based fiber devices have been developed, with important applications in the area such as RI sensing [5–10].

Fiber Bragg grating (FBG) is one of the basic optical fiber components that have wide applications. However, FBG is intrinsically insensitive to the external RI change, as it is not directly exposed to the surrounding medium. Although such a difficulty can be alleviated by thinning or etching of the fiber after the FBG creation [11–13], the mechanical strength and durability of the sensing device are greatly reduced, which limits the applications of FBG-based RI sensors. In contrast, long period fiber grating (LPFG) is widely used as the RI sensor, owing to its intrinsically high sensitivity to the surrounding medium change in a large range [14]. However, the transmission dips of the LPFG are broad (typical of tens of nanometers) [12], resulting in a poor measurement accuracy. Meanwhile, the length of the LPFG is relatively large (typical of  $\sim 30$  mm) [15], which limits its applications in accurate sensor devices.

The FBG in microfiber can overcome the above-mentioned difficulties because of its narrow bandwidth, small grating size, and good measurement accuracy. Moreover, the FBG can support the multi-

plexed system, showing significant advantages over the LPFG.

A powerful tool for the FBG fabrication is a femtosecond laser, which allows the inscription of the FBG in almost any type of optical fibers without photosensitivity [16,17]. Because of the extremely large light intensity across a small spatial region and ultrashort interaction time, the RI change induced by the high-power femtosecond laser pulses is highly localized, which supports the fabrication of strong and high-spectral-quality FBGs. To the best of our knowledge, no FBG has been fabricated in a microfiber yet.

In this Letter, we present the successful FBG fabrication by the use of femtosecond pulse irradiation in microfibers with diameters ranging from 2 to 10  $\mu\text{m}$ . Such a FBG can be directly exposed to the surrounding medium without etching or thinning treatment of the fiber, representing an easy and convenient way of achieving high sensitivity measurement while retaining wavelength encoded measurement information.

The microfiber is produced by the use of flame brushing method in a simple optical coupler manufacturing system (OC 2010) [2,18,19], where a small flame moves slowly under a single-mode fiber stretched by two moving vacuum absorption holders. The torch flame intensity can be adjusted by controlling the flux of  $\text{H}_2$ , which is optimized at approximately 134 standard cubic centimeters per minute in our experiment, just enough to support the flame to soften the glass without inducing a large loss. The scanning length of the torch is  $\sim 7$  mm, which limits the fiber length. The relative speed of the torch and holders plays an important role in the formation of the microfiber and its insertion loss. If the speed is too high, the fiber diameter becomes large, owing to the limited softening time of the fiber. When the speed is too low, a high insertion loss will result, owing to the large fiber deformation. Thus, by appropriately controlling the speed of the flame and the hold-

ers, microfibers of different diameters exhibiting a loss of less than 0.1 dB can be achieved.

The femtosecond laser used for the FBG fabrication is a Ti:sapphire laser system consisting of an oscillator (Mai Tai) and an amplifier (Spitfire Pro). The output pulse duration is 120 fs, with a repetition rate of 1 kHz at 800 nm. The laser exposure time is less than 10 s, and the pulse energy can be adjusted from 150 to 200  $\mu\text{J}$  by rotating a half-wave plate followed by a linear polarizer. During the FBG fabrication, the microfiber is placed in front of a chirped phase mask (Stocker Yale) with a chirp rate of 4.8 nm/cm and the period of 2149.95 nm. The FBGs fabricated have a length of  $\sim 4$  mm, determined by the laser spot size of  $\sim 5$  mm (the energy at the edge of the spot is too weak to form a grating). The microscope image of the FBG fabricated in the microfiber with diameter of 10  $\mu\text{m}$  is shown in Fig. 1.

Figure 2 demonstrates the reflection spectra of the FBGs in the microfibers with different diameters down to 2  $\mu\text{m}$ . The optical spectrum analyzer used has the resolution of 0.01 nm. It can be seen from the figure that the center wavelength of the FBG is blue-shifted with the decrease in the fiber diameter, as more propagating mode energy goes outside the fiber, causing the reduction in the fiber effective RI [11]. The 3 dB bandwidth of the FBG varies from 0.67 to 1.79 nm, owing to the variation of fabrication conditions such as the changes in the fiber position, laser exposure time, and the chirped phase mask used.

Figure 3 shows the transmission spectrum of the FBG with a diameter of 10  $\mu\text{m}$ . Compared with its reflection spectrum shown in Fig. 2, where only one fundamental resonance mode appears, nine modes exist in the same wavelength range between 1512 and 1562 nm. The small burrs near the resonance modes may be due to the chirped phase mask used.

It can be noted that the mode at 1548 nm in Fig. 2 is the fundamental mode, while mode 5 at 1536 nm in Fig. 3 is the higher mode, which can hardly be observed in the reflection spectrum. Actually, the coupling coefficient of each mode is dependent on the relative position between the fiber and the laser spot. In our experiment, the laser may not be focused at the center of the fiber when the fiber is slightly tilted, which makes the strongest resonance wavelength fall into the fifth mode.

The RI measurement by the use of the FBG in microfiber is carried out at the room temperature by immersing the FBG into the liquid with RI values varying from 1.32 to 1.46. Each time after the mea-

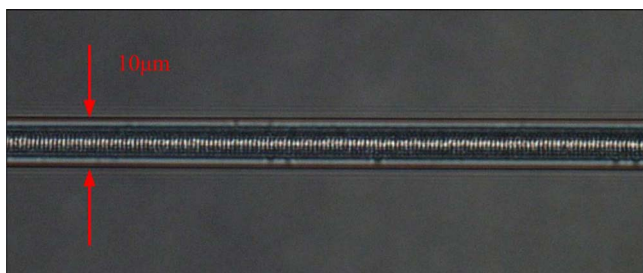


Fig. 1. (Color online) Microscope image of the microfiber with diameter of  $\sim 10$   $\mu\text{m}$ .

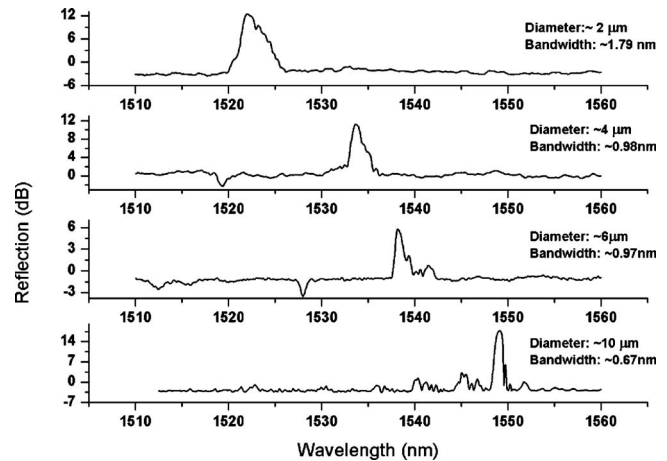


Fig. 2. Reflection spectra of the FBGs in microfiber with diameters of 2, 4, 6, and 10  $\mu\text{m}$ .

surement, the device is rinsed with methanol carefully until the original spectrum is restored and no residual liquid is left. To observe the resonance wavelength of all the modes, the transmission spectrum is monitored. Figure 4 shows the redshift of the transmission wavelengths when the ambient RI increases. When the RI is close to the fiber index value, a relatively high sensitivity can be obtained, owing to the enhanced influence of the external RI on the propagation mode, which becomes less confined in the fiber. The RI measurement range of our FBG is limited by the fiber material, i.e.,  $n_{\text{max}} = 1.46$  for the glass fiber. If a larger range is needed, the fiber material with a higher RI has to be used.

The higher-order mode has more energy distributed outside the fiber, thus exhibiting the higher sensitivity to the ambient RI. Figure 5 shows the RI sensitivity for different orders of fiber mode when the fiber diameter is  $\sim 10$   $\mu\text{m}$ . The sensitivity is obtained by calculating the first-order derivative of the wavelength shift shown in Fig. 4, followed by an exponential curve fitting. According to Fig. 5, with the same ambient RI, the higher-order resonance mode has higher sensitivity compared with the lower-order mode. The maximum sensitivity obtained

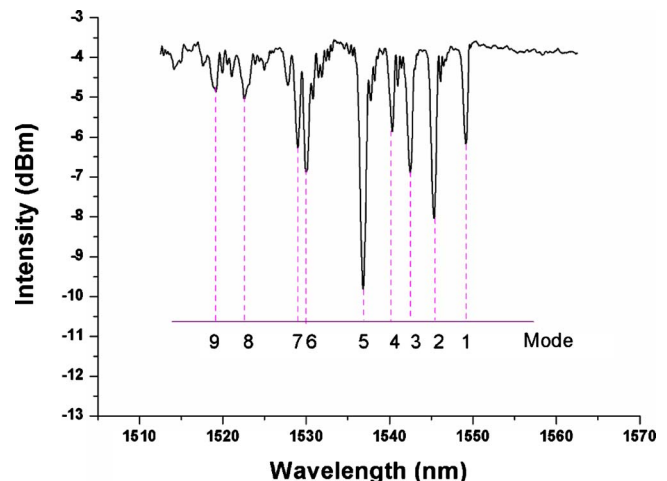


Fig. 3. (Color online) Transmission spectrum of the FBG in microfiber with diameter of  $\sim 10$   $\mu\text{m}$ .

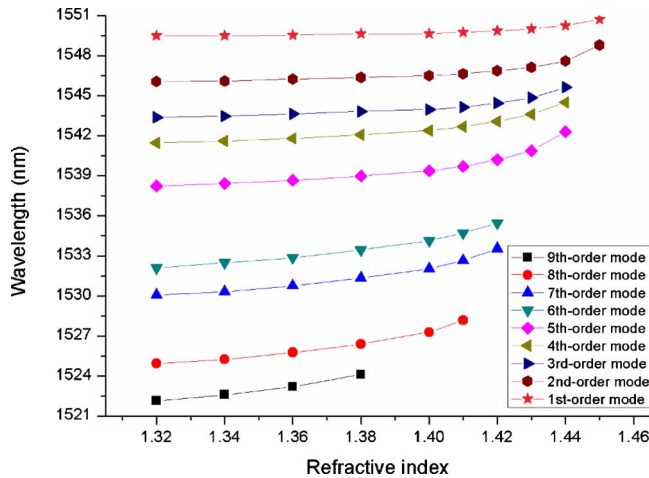


Fig. 4. (Color online) Wavelength change with the external RI at different orders of resonance mode.

is  $\sim 184.6$  nm per refractive index unit (RIU), for the fifth-order mode, at the RI value of 1.44. Some higher-order modes are disappeared or hardly observed when the ambient RI is increased, as the resonance effect is reduced owing to the less propagation mode energy confined in the fiber.

The RI sensitivity also depends on the fiber diameter and is increased when a smaller fiber diameter is used. The maximum sensitivity obtained is  $\sim 231.4$  nm/RIU at the RI value of 1.44, corresponding to the fiber diameter of  $\sim 2$   $\mu\text{m}$ , as shown in Fig. 6.

In conclusion, what we believe to be a novel FBG in microfiber is fabricated by the use of femtosecond laser pulse irradiation. Such an FBG can be directly exposed to the surrounding medium without etching or thinning treatment of the fiber and has high RI sensitivity especially when the higher order of fiber mode is utilized. The maximum sensitivity obtained for the first order mode is  $\sim 231.4$  nm/RIU, at the RI value of  $\sim 1.44$ , when the fiber diameter is  $\sim 2$   $\mu\text{m}$ .

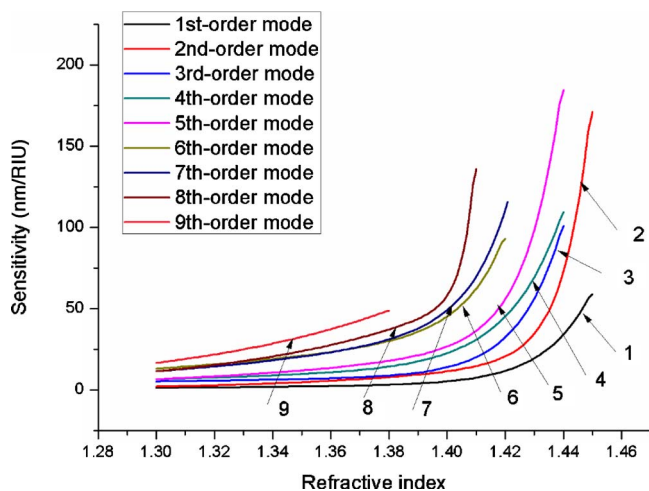


Fig. 5. (Color online) RI sensitivity of different orders of mode for the FBG in microfiber with diameter of  $\sim 10$   $\mu\text{m}$ .

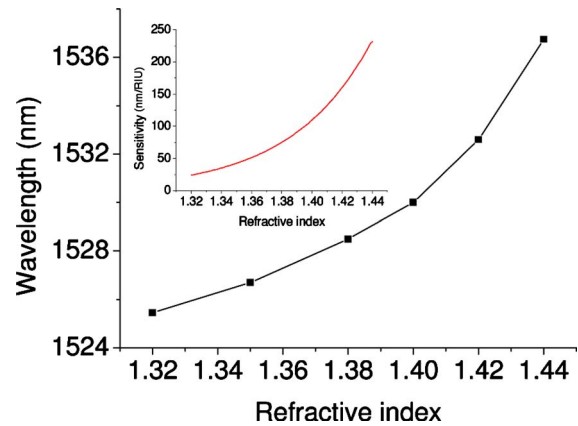


Fig. 6. (Color online) Wavelength change with the external RI at different orders of resonance mode. Inset, RI sensitivity of different orders of mode for the FBG in microfiber with diameter of  $\sim 2$   $\mu\text{m}$ .

The FBG in microfiber has high potential in the RI measurement and other optical fiber sensor applications. The FBG fabrication method developed in this work is also applicable to inscribe the FBG in nanofibers.

## References

1. L. Tong, R. R. Gattass, J. B. Ashcom, S. He, J. Lou, M. Shen, I. Maxwell, and E. Mazur, *Nature* **426**, 816 (2003).
2. G. Brambilla, V. Finazzi, and D. Richardson, *Opt. Express* **12**, 2258 (2004).
3. M. Sumetsky, Y. Dulashko, and A. Hale, *Opt. Express* **12**, 3521 (2004).
4. S. Leon-Saval, T. Birks, W. Wadsworth, P. St. J. Russell, and M. Mason, *Opt. Express* **12**, 2864 (2004).
5. P. Polynkin, A. Polynkin, N. Peyghambarian, and M. Mansuripur, *Opt. Lett.* **30**, 1273 (2005).
6. F. Xu, P. Horak, and G. Brambilla, *Opt. Express* **15**, 7888 (2007).
7. M. Sumetsky, R. S. Windeler, Y. Dulashko, and X. Fan, *Opt. Express* **15**, 14376 (2007).
8. M. Sumetsky, *J. Lightwave Technol.* **26**, 21 (2008).
9. X. Jiang, Y. Chen, G. Vienne, and L. Tong, *Opt. Lett.* **32**, 1710 (2007).
10. Y. Li and L. Tong, *Opt. Lett.* **33**, 303 (2008).
11. A. Iadicicco, A. Cusano, A. Cutolo, R. Bernini, and M. Giordano, *IEEE Photon. Technol. Lett.* **16**, 1149 (2004).
12. W. Liang, Y. Huang, Y. Xu, R. K. Lee, and A. Yariv, *Appl. Phys. Lett.* **86**, 151122 (2005).
13. A. N. Chryssis, S. M. Lee, S. B. Lee, S. S. Saini, and M. Dagenais, *IEEE Photon. Technol. Lett.* **17**, 1253 (2005).
14. H. J. Patrick, A. D. Kersey, and F. Bucholtz, *J. Lightwave Technol.* **16**, 1606 (1998).
15. S. W. James and R. P. Tatam, *Meas. Sci. Technol.* **14**, R49 (2003).
16. C. Florea and K. A. Winick, *J. Lightwave Technol.* **21**, 246 (2003).
17. S. J. Mihailov, C. W. Smelser, D. Grobncic, R. B. Walker, P. Lu, H. Ding, and J. Unruh, *J. Lightwave Technol.* **22**, 94 (2004).
18. Y. Lizé, E. Mägi, V. Ta'eed, J. Bolger, P. Steinvurzel, and B. Eggleton, *Opt. Express* **12**, 3209 (2004).
19. F. Bilodeau, K. O. Hill, S. Faucher, and D. C. Johnson, *J. Lightwave Technol.* **6**, 1476 (1988).